

Time-Scale Coupling Between States and Parameters in Recurrent Neural Networks*

Lorenzo Livi*

August 19, 2025

Abstract

We study how gating mechanisms in recurrent neural networks (RNNs) implicitly induce adaptive learning-rate behavior, even when training is carried out with a fixed, global learning rate. This effect arises from the coupling between state-space time scales—parametrized by the gates—and parameter-space dynamics during gradient descent. By deriving exact Jacobians for leaky-integrator and gated RNNs, we obtain a first-order expansion that makes explicit how constant, scalar, and multi-dimensional gates reshape gradient propagation, modulate effective step sizes, and introduce anisotropy in parameter updates. These findings reveal that gates not only control memory retention in the hidden states, but also act as data-driven preconditioners that adapt optimization trajectories in parameter space. We further draw formal analogies with learning-rate schedules, momentum, and adaptive methods such as Adam, showing that these optimization behaviors emerge naturally from gating. Numerical experiments confirm the validity of our perturbative analysis, supporting the view that gate-induced corrections remain small while exerting systematic effects on training dynamics. Overall, this work provides a unified dynamical-systems perspective on how gating couples state evolution with parameter updates, explaining why gated architectures achieve robust trainability and stability in practice.

Contents

1	Introduction	2
2	Related Works	3
3	RNNs and Time-Scales	4
3.1	From Continuous to Discrete Time	4
3.2	Global Time Rescaling	5
3.3	General Time Warping and Gating	5
4	BPTT-based training of RNNs	6
4.1	Gradient descent in neural networks	6
4.2	Vanishing and exploding gradients	7
5	How time-scales in RNN states affect parameter dynamics	7
5.1	Jacobian matrices	8
5.1.1	Leaky-integrator neurons	8
5.1.2	Single scalar gate	8
5.1.3	Multiple gates	8
5.2	Time-scale interaction	9

*OPIT – Open Institute of Technology, lorenz.livi@gmail.com

5.2.1	Constant gate case	9
5.2.2	RNNs with scalar gate	9
5.2.3	RNNs with multiple gates	11
6	Gradient descent algorithms	12
6.1	Adam	13
6.2	Analogies between gating mechanisms and adaptive gradient descent methods	13
7	Conclusions and future directions	14
A	Matrix product expansion via the Fréchet derivative formulation	15
A.1	Fréchet Differentiability and the First-Order Expansion	15
A.2	Matrix products with structured perturbations	16
A.3	Recursive application of the product rule	16
A.4	First-order expansion	17
A.5	Simulations supporting the validity of the first-order approximation	18

1 Introduction

Recurrent neural networks (RNNs) remain a fundamental tool for modeling sequential data, yet their training dynamics continue to present theoretical and practical challenges. While much progress has been made in designing architectures that mitigate gradient pathologies, improve stability, or enhance memory retention, a unified understanding of how state dynamics and parameter updates interact—particularly under the influence of gating—remains incomplete. In many modern architectures, gates act not only as information filters but also as modulators of time scales in the underlying dynamics. This dual role raises important questions about how gating shapes both the short-term evolution of hidden states and the long-term trajectory of parameters during optimization.

In this work, we show that gating mechanisms have a further, often overlooked effect: they implicitly induce *adaptive learning-rate behavior*, even when training is performed with a static, fixed global learning rate. This phenomenon arises because the same time-scale modulations that gates impose on state dynamics directly couple into the parameter-update dynamics via backpropagation. In other words, the gates do not merely control information flow in the hidden states; they also reshape the effective optimization process in parameter space, altering step sizes, scaling directions, and introducing anisotropy in the updates.

Our analysis is grounded in a perturbative expansion of the Jacobian products arising in backpropagation, which makes these effects explicit. We derive exact Jacobians for leaky-integrator, scalar-gated, and multi-gated RNNs, and show how their influence on state transitions translates into systematic modifications of parameter-space dynamics. This perspective reveals clear analogies with gradient descent algorithms such as SGD with learning rate schedules, momentum, and adaptive methods like Adam. Importantly, these behaviors emerge endogenously from the gating dynamics, rather than from externally imposed optimization heuristics.

Beyond theoretical analysis, we validate our assumptions and approximations through numerical experiments on RNNs with different gating configurations. These experiments confirm the accuracy of the first-order Jacobian expansion in both small-perturbation and practical operating regimes, supporting the conclusion that gates exert structured but bounded corrections to the dominant state-transition dynamics. Taken together, our findings provide a unified dynamical-systems perspective on how gating couples state evolution with parameter updates, explaining why gated architectures achieve robust trainability and stability in practice.

The main contributions of this paper are:

- We present a unified theoretical framework that explains how gates implicitly induce adaptive learning-rate effects in parameter space, even under a fixed global learning rate, by coupling state-space time scales with parameter dynamics.

- We derive explicit Jacobian-based perturbative expansions for constant, scalar, and multi-dimensional gates, linking their influence to gradient propagation, anisotropy in parameter updates, and memory retention.
- We establish formal analogies between gating-induced effects and optimization algorithms, including learning-rate schedules, momentum, and adaptive methods such as Adam.
- We validate our theoretical framework with numerical experiments, confirming both the smallness of gate-induced corrections and the robustness of the first-order approximation.

The remainder of the paper is organized as follows. Section 2 surveys the most relevant literature on gradient pathologies, linear and state-space models, constrained recurrent dynamics, and gating mechanisms. Section 3 introduces the interpretation of RNN gating mechanisms as parametrized time-scales and formalizes the specific models considered in our analysis. Section 4 reviews backpropagation through time in RNNs and revisits the vanishing/exploding gradient problem in this context. Section 5 presents our main contribution: we derive the Jacobian matrices for the considered RNN models and show how state-space time-scales influence the behaviour of gradient descent, thereby revealing the interaction between state and parameter dynamics. Section 6 discusses well-known variants of gradient descent and establishes explicit connections between their behaviour and the effects induced by gating mechanisms. Finally, Section 7 summarizes the key findings and outlines future research directions, including the extension of our framework to more advanced gated architectures such as LSTMs and GRUs.

2 Related Works

The study of recurrent neural networks (RNNs) has long been shaped by the well-known vanishing and exploding gradient problem [21], which affects the stability and learnability of long-term dependencies. While this issue traditionally focuses on the magnitude of gradients, recent work by Zucchetti and Orvieto [34] highlights a complementary phenomenon: as the memorization capacity of an RNN increases during training, the network output can become highly sensitive to small parameter variations. This heightened sensitivity arises even in the absence of vanishing or exploding gradients, suggesting that RNNs may undergo abrupt changes in behavior due to intrinsic instabilities in the learned parameter–state mapping. In a related vein, Cen et al. [3] proposed Random Orthogonal Additive Filters, a class of architectures designed to stabilize and enrich recurrent dynamics via orthogonal transformations, mitigating instability without sacrificing representational power.

Several lines of research have explored simplified linear models as a means of studying and designing recurrent dynamics with greater interpretability. Continuous-time state-space models, such as those in Gu et al. [8, 9], have enabled efficient training of sequence models with long-range dependencies by leveraging structured state-space kernels. More recently, Muca Cirone et al. [20] provided a theoretical analysis of linear state-space models (LSSMs), clarifying their expressive power and the role of parameterization in controlling stability and memory retention. These models offer a valuable bridge between classical control theory and modern deep learning approaches to sequence modeling.

From a training dynamics perspective, Lee et al. [18] analyzed wide neural networks through the lens of the neural tangent kernel, providing insights into the coupling between parameters and outputs during optimization. Although this framework is often applied to feedforward networks, it has implications for understanding the parameter–state interaction in recurrent settings, particularly in regimes where network width and gating jointly influence effective learning rates. Complementary work by Saxe et al. [27] investigated exact learning dynamics in deep linear networks, showing how singular value spectra dictate timescales of parameter evolution. This resonates with our perspective that recurrent gates modulate effective timescales in both state and parameter spaces.

Another rich research area involves constraining recurrent weight matrices to improve stability, expressivity, or trainability. Orthogonal and unitary RNNs [1, 10, 19, 31, 33] maintain constant gradient norms over time, thus alleviating the vanishing/exploding gradient problem. Lipschitz RNNs [6] extend this idea by

explicitly controlling the Lipschitz constant to ensure robustness. Non-normal RNNs [14] and their variants incorporating Schur decompositions [13] have been proposed to exploit transient amplification phenomena for richer dynamics. Other designs include antisymmetric RNNs [4], which draw inspiration from Hamiltonian systems to ensure stability, coupled RNNs [25], which model interacting subsystems, and multiscale RNNs [26], which embed explicit time-scale separation into the architecture. Related architectural innovations such as the Clockwork RNN [16] also demonstrate the utility of explicitly incorporating multiple timescales into recurrent dynamics.

Gating mechanisms have received particular attention for their role in modulating information flow and improving trainability. From a theoretical standpoint, Chen et al. [5] and Gilboa et al. [7] analyzed the effects of gating on dynamical isometry and mean-field properties in RNNs, showing that gates can help preserve gradient flow and condition the optimization landscape. Related analyses in feedforward networks [22] underline the generality of dynamical isometry principles across architectures. Architecturally, stacked gated RNNs [29] and hybrid designs such as the “Just Another Network” (JANET) [30] demonstrate the versatility of gating in achieving both memory retention and efficient optimization. More recent theoretical work further strengthens this connection: Krishnamurthy et al. [17] and Can et al. [2] showed that gates can create slow modes in recurrent dynamics, directly modulating Jacobian spectra and shaping effective memory timescales. Empirical studies such as Quax et al. [23] confirmed that RNNs tend to develop adaptive timescales when trained on multi-scale sequential data, further illustrating the deep connection between gating and temporal structure.

In contrast to these prior works, which often study either stability, memory, or optimization in isolation, our work examines the *joint* dynamics of states and parameters under the influence of gating. By framing gating as a parametrized time-scale modulation and applying perturbative analysis to the Jacobian products that arise in backpropagation, we connect architectural design choices directly to their effect on parameter update anisotropy, gradient scaling, and memory retention across time scales.

3 RNNs and Time-Scales

We begin with a simple continuous-time RNN model [28]:

$$\frac{dx(t)}{dt} = \phi(W^r x(t) + W^i u(t)) - x(t), \quad x(0) = x_0, \quad (1)$$

where the state vector $x(t) \in \mathbb{R}^{N_r}$ evolves under the recurrent weights $W^r \in \mathbb{R}^{N_r \times N_r}$, input weights $W^i \in \mathbb{R}^{N_r \times N_i}$, and elementwise nonlinearity $\phi(\cdot)$.

The output is generated via a readout mapping

$$z(t) = \psi(x(t)), \quad (2)$$

which, in the common linear case, reduces to

$$z(t) = W^o x(t), \quad W^o \in \mathbb{R}^{N_o \times N_r}. \quad (3)$$

Different readout functions $\psi(\cdot)$ may be chosen depending on the task.

3.1 From Continuous to Discrete Time

Applying a first-order Taylor expansion around t (i.e., Euler discretization) to (1) gives

$$x(t + \delta t) \approx x(t) + \delta t \frac{dx(t)}{dt}. \quad (4)$$

With unit step $\delta t = 1$, this yields the standard discrete-time RNN update

$$x_{t+1} = \phi(W^r x_t + W^i u_t), \quad (5)$$

with discrete-time output

$$z_t = \psi(x_t), \quad (6)$$

and, in the linear case,

$$z_t = W^o x_t. \quad (7)$$

3.2 Global Time Rescaling

Suppose we want to model a time-rescaled input $u(\alpha t)$ with (1). Let the state trajectory be reparameterized as $x(\alpha t)$ via a linear time-warping function

$$c(t) = \alpha t, \quad \alpha > 0. \quad (8)$$

Rewriting (1) with the new time variable, $T = c(t) = \alpha t$, we obtain:

$$\frac{dx(c(t))}{dt} = \frac{dx(T)}{dT} \frac{dT}{dt} = \alpha \phi(W^r x(t) + W^i u(t)) - \alpha x(t), \quad (9)$$

where we have renamed $t = T$ on the right-hand side to simplify the notation. This expression shows that a time-warping $c(t) = \alpha t$ scales both the recurrent and decay terms by the same factor α . Therefore, the original dynamics in (1) are *not* invariant under time-rescaling: the evolution is accelerated for $\alpha > 1$ and slowed down for $\alpha < 1$. In this sense, α acts as a global update rate, with $\alpha \rightarrow 0$ yielding nearly frozen dynamics and $\alpha \rightarrow \infty$ corresponding to very fast updates.

Discretizing (9) with (4) and $\delta t = 1$ yields

$$x_{t+1} = \alpha \phi(W^r x_t + W^i u_t) + (1 - \alpha)x_t, \quad (10)$$

which corresponds to *leaky integrator* neurons [12]. Here α is the *global state-update rate*, and its reciprocal $\tau = 1/\alpha \in [1, \infty)$ defines the global discrete-time scale. When $\alpha \rightarrow 0$, state updates occur very slowly, approaching a static memory.

3.3 General Time Warping and Gating

To go beyond global rescaling and achieve invariance to more general time transformations, we allow an arbitrary *monotonic, differentiable* warping $c : \mathbb{R} \rightarrow \mathbb{R}$.

$$\frac{dx(c(t))}{dt} = \frac{dc(t)}{dt} \phi(W^r x(t) + W^i u(t)) - \frac{dc(t)}{dt} x(t), \quad (11)$$

$$= g(t) \phi(W^r x(t) + W^i u(t)) - g(t) x(t), \quad (12)$$

where

$$g(t) := \frac{dc(t)}{dt} \quad (13)$$

is the instantaneous *state-update rate*. When $g(t) \equiv \alpha$, we recover the leaky case (9).

We parametrize $g(t)$ as a *gate*:

$$g(t) = \sigma(W^{r,g} x(t) + W^{i,g} u(t)), \quad (14)$$

where $\sigma(\cdot) \in (0, 1)$ is the logistic sigmoid, $W^{r,g} \in \mathbb{R}^{1 \times N_r}$, and $W^{i,g} \in \mathbb{R}^{1 \times N_i}$ are gate parameters. This parametrization ensures that the update rate $g(t)$ remains bounded in $(0, 1)$, thereby smoothly interpolating between two extremes: $g(t) \approx 0$ corresponds to almost frozen dynamics (long time scale), while $g(t) \approx 1$ yields rapid updates (short time scale). Because $g(t)$ depends both on the current state $x(t)$ and the input $u(t)$, the effective time scale of the network becomes data- and state-dependent. This means that the model can adaptively modulate its temporal resolution on the fly, allocating fast or slow dynamics depending on the context, rather than relying on a fixed global constant α as in the leaky-integrator case.

Discretizing (12) with $\delta t = 1$ gives

$$x_{t+1} = g_t \phi(W^r x_t + W^i u_t) + (1 - g_t) x_t, \quad (15)$$

which makes the dynamics invariant to a global rescaling of time and, more generally, allows them to adapt to smoothly varying changes in the time axis through the gate g_t .

For neuron-specific time scales, we assign an individual gate $g_t^{(j)}$ to each neuron j :

$$x_{t+1} = g_t \odot \phi(W^r x_t + W^i u_t) + (1 - g_t) \odot x_t, \quad (16)$$

where \odot denotes elementwise multiplication and

$$g_t = \begin{bmatrix} g_t^{(1)} \\ \vdots \\ g_t^{(N_r)} \end{bmatrix} \in (0, 1)^{N_r}. \quad (17)$$

Here $\sigma(\cdot)$ in (14) is applied componentwise, with $W^{r,g} \in \mathbb{R}^{N_r \times N_r}$ and $W^{i,g} \in \mathbb{R}^{N_r \times N_i}$. Each neuron thus possesses its own *time-dependent update rate* (or time scale), enabling fine-grained adaptation of the network's temporal dynamics.

4 BPTT-based training of RNNs

4.1 Gradient descent in neural networks

The most basic form of the gradient descent (GD) update rule for a parameter vector θ using a mini-batch of size $b \geq 1$ is

$$\theta_{l+1} = \theta_l - \frac{\mu}{b} \sum_{t=1}^b \frac{\partial \mathcal{E}_t}{\partial \theta_l}, \quad (18)$$

where l indexes the training iteration, $\mu > 0$ is the learning rate (or step size), and \mathcal{E}_t is the loss at sample t in the mini-batch. For instance, in a regression setting one may use the squared error

$$\mathcal{E}_t = \|y_t - z_t\|^2,$$

where y_t is the target output, $z_t = f(\cdot; \theta)$ is the model prediction (combining the state-update and output mappings), and θ collects all trainable parameters of the network.

The gradient $\frac{\partial \mathcal{E}_t}{\partial \theta_l}$ in (18) can be expanded using the chain rule. For recurrent models, the dependence of the current state x_t on all previous states $\{x_k\}_{k < t}$ must be taken into account:

$$\sum_{t=1}^b \frac{\partial \mathcal{E}_t}{\partial \theta_l} = \sum_{t=1}^b \frac{\partial \mathcal{E}_t}{\partial x_t} \sum_{k=1}^t \frac{\partial x_t}{\partial x_k} \frac{\partial x_k}{\partial \theta_l}. \quad (19)$$

Here, the term $\frac{\partial x_t}{\partial x_k}$ is the product of Jacobian factors linking the state at time t to the state at time k , which makes the computation inherently sequential.

Because the error gradients must be propagated backward through the sequence of states, this procedure is known as *backpropagation*. When applied to recurrent neural networks, where parameters are shared across time steps, the method is referred to as *backpropagation through time* (BPTT) [32].

4.2 Vanishing and exploding gradients

A central difficulty in computing (19) arises from the presence of long products of Jacobian matrices. For any $k < t$, the sensitivity of x_t with respect to x_k is given by

$$\frac{\partial x_t}{\partial x_k} = \prod_{j=k+1}^t J_j, \quad (20)$$

$$J_j = \frac{\partial x_j}{\partial x_{j-1}}, \quad (21)$$

where J_j is the Jacobian of the state update at time j .

Using the submultiplicative property of matrix norms,

$$\left\| \frac{\partial x_t}{\partial x_k} \right\| \leq \prod_{j=k+1}^t \|J_j\|, \quad (22)$$

and substituting into (19) gives the following bound on the gradient norm:

$$\left\| \frac{\partial \mathcal{E}_t}{\partial \theta_l} \right\| \leq \left\| \frac{\partial \mathcal{E}_t}{\partial x_t} \right\| \prod_{j=k+1}^t \|J_j\|. \quad (23)$$

Consider now the standard discrete-time RNN model (5). The Jacobian at step j has the form

$$J_j = D_{j-1} W^r, \quad (24)$$

where

$$D_j = \text{diag}(\phi'(a_j)) \quad (25)$$

is a diagonal matrix containing the derivatives of the activation function ϕ evaluated at the pre-activation

$$a_{j-1} = W^r x_{j-1} + W^i u_{j-1}. \quad (26)$$

In this case, (22) specializes to

$$\prod_{j=k+1}^t \|D_{j-1}\| \|W^r\|. \quad (27)$$

From (27), it is clear that if the spectral norm $\|W^r\|$ or the activation derivatives $\|D_{j-1}\|$ are consistently smaller than 1, the product will decay exponentially with $(t - k)$, leading to *vanishing gradients*. Conversely, if either factor is consistently greater than 1, the product will grow exponentially, producing *exploding gradients*. This spectral-norm dependence of the gradient magnitude is well documented in the literature [21] and motivates many of the stability constraints and reparameterizations used in modern RNN architectures.

5 How time-scales in RNN states affect parameter dynamics

In Section 5.1, we derive the exact expressions for the Jacobian matrices associated with the RNN variants introduced in Section 3. These Jacobians govern how perturbations to the hidden state propagate through time, and thus play a central role in both forward signal evolution and backward gradient flow. Building on these results, Section 5.2 analyzes how the time-scales embedded in the state-space dynamics interact with the optimization process. In particular, we show how the presence of constant, scalar, or multiple gating mechanisms influences the effective learning rate and the direction of parameter updates, thereby shaping the behaviour of the gradient descent algorithm.

5.1 Jacobian matrices

5.1.1 Leaky-integrator neurons

For the leaky-integrator model (10), the Jacobian at time j is

$$J_j = \alpha D_{j-1} W^r + (1 - \alpha) I, \quad (28)$$

where I is the identity matrix and $D_{j-1} = \text{diag}(\phi'(a_{j-1}))$ (see (25)). Relative to the standard RNN Jacobian $D_{j-1} W^r$, the constant gate α scales the recurrent contribution while adding a skip connection proportional to $(1 - \alpha)I$, thereby tempering gradient decay or explosion.

5.1.2 Single scalar gate

Consider now the scalar-gated model (15). Defining the gate pre-activation

$$a_t^g = W^{r,g} x_t + W^{i,g} u_t \in \mathbb{R}, \quad (29)$$

the Jacobian becomes

$$J_j = \left[\phi(a_{j-1}) \frac{\partial g_{j-1}}{\partial x_{j-1}} + g_{j-1} D_{j-1} W^r \right] + \left[x_{j-1} \frac{\partial(1 - g_{j-1})}{\partial x_{j-1}} + (1 - g_{j-1}) I \right] \quad (30)$$

$$= (\phi(a_{j-1}) - x_{j-1}) J_{j-1}^g + g_{j-1} D_{j-1} W^r + (1 - g_{j-1}) I \quad (31)$$

$$= G_{j-1} + g_{j-1} D_{j-1} W^r + (1 - g_{j-1}) I, \quad (32)$$

where

$$J_j^g = \frac{\partial g_j}{\partial x_j} = \sigma'(a_j^g) W^{r,g}, \quad G_{j-1} = d_{j-1} J_{j-1}^g, \quad d_{j-1} = \phi(a_{j-1}) - x_{j-1}. \quad (33)$$

Here $J_j^g \in \mathbb{R}^{1 \times N_r}$ and G_{j-1} is rank-1, being the outer product of d_{j-1} and J_{j-1}^g . Thus, the scalar gate introduces a low-rank correction G_{j-1} in addition to rescaling the recurrent and skip terms.

5.1.3 Multiple gates

For the multi-gated model (16), the gate pre-activation is a vector $a_j^g \in \mathbb{R}^{N_r}$, yielding the Jacobian

$$J_j^g = \frac{\partial g_j}{\partial x_j} = \text{diag}(\sigma'(a_j^g)) W^{r,g} = D_j^g W^{r,g}, \quad (34)$$

with $D_j^g = \text{diag}(\sigma'(a_j^g))$. In this case, $g_j \in \mathbb{R}^{N_r}$ is a vector of unit-wise update rates.

Introducing the shorthand $\hat{d} = \text{diag}(d)$ for a diagonal matrix with vector d on the diagonal, and $\hat{g} = I - \hat{g}$, the Jacobian reads

$$J_j = \hat{\phi}(a_{j-1}) J_{j-1}^g + \hat{g}_{j-1} D_{j-1} W^r - \hat{x}_{j-1} J_{j-1}^g + \hat{g}_{j-1} I \quad (35)$$

$$= \hat{d}_{j-1} J_{j-1}^g + \hat{g}_{j-1} D_{j-1} W^r + \hat{g}_{j-1} I \quad (36)$$

$$= G_{j-1} + \hat{g}_{j-1} D_{j-1} W^r + \hat{g}_{j-1} I. \quad (37)$$

Unlike the scalar case, here G_{j-1} is not rank-deficient, since it results from multiplying a diagonal matrix by a full matrix.

5.2 Time-scale interaction

In this section, we show that the interaction between state-space time scales and parameter updates gives rise to an *effective learning rate* μ^* , which generally differs from the nominal learning rate μ in (18). The precise form of μ^* depends on the chosen state-space model. To this end, without loss of generality we consider only time-step t and expand the gradient formula in (19) as follows:

$$\frac{\partial \mathcal{E}_t}{\partial \theta_l} = \frac{\partial \mathcal{E}_t}{\partial x_t} \sum_{k=1}^t \left[\prod_{j=k+1}^t J_j \right] \frac{\partial x_k}{\partial \theta_l}. \quad (38)$$

5.2.1 Constant gate case

In the constant gate case $g_t \equiv \alpha \in (0, 1]$, the Jacobian (28) is

$$J_j = I + \alpha A_{j-1}, \quad A_{j-1} := D_{j-1}W_r - I. \quad (39)$$

The BPTT gradient can then be written as

$$\frac{\partial E_t}{\partial \theta_l} = \frac{\partial E_t}{\partial x_t} \sum_{k=1}^t \left[\prod_{j=k+1}^t (I + \alpha A_{j-1}) \right] \frac{\partial x_k}{\partial \theta_l}, \quad (40)$$

where θ_l denotes any parameter of the network (weights, biases, gating parameters, etc.).

Factoring α out of each Jacobian in the product gives

$$\prod_{j=k+1}^t (I + \alpha A_{j-1}) = \left(\prod_{j=k+1}^t \alpha \right) \prod_{j=k+1}^t (\alpha^{-1}I + A_{j-1}) = \alpha^{t-k} \mathcal{P}_{t,k}, \quad (41)$$

where we defined the normalized product

$$\mathcal{P}_{t,k} := \prod_{j=k+1}^t (\alpha^{-1}I + A_{j-1}). \quad (42)$$

Substituting back, the gradient becomes

$$\frac{\partial E_t}{\partial \theta_l} = \frac{\partial E_t}{\partial x_t} \sum_{k=1}^t \alpha^{t-k} \mathcal{P}_{t,k} \frac{\partial x_k}{\partial \theta_l}. \quad (43)$$

The factor α^{t-k} is the exact multiplicative decay applied to gradient components that travel through $(t-k)$ recurrent steps. This is equivalent to saying that during BPTT there is no “global” learning rate μ , but an “effective” learning rate that is valid in the time lag $t-k$. The effective learning rate reads:

$$\mu_{t,k}^* = \mu \alpha^{t-k}. \quad (44)$$

This makes explicit that the learning rate decays exponentially with temporal distance, at a rate fully determined by α . For $\alpha < 1$, long-range dependencies are progressively downweighted, leading to a vanishing gradient phenomenon for long temporal distances.

5.2.2 RNNs with scalar gate

When considering the Jacobian in (32), the product of Jacobians inside the gradient update formula can be rewritten as:

$$\prod_{j=k+1}^t G_{j-1} + g_{j-1} D_{j-1} W^r + (1 - g_{j-1}) I = \prod_{j=k+1}^t G_{j-1} + I + g_{j-1} (D_{j-1} W^r - I). \quad (45)$$

The gradient equation becomes:

$$\frac{\partial \mathcal{E}_t}{\partial \theta_l} = \frac{\partial \mathcal{E}_t}{\partial x_t} \sum_{k=1}^t \left[\prod_{j=k+1}^t G_{j-1} + I + g_{j-1}(D_{j-1}W^r - I) \right] \frac{\partial x_k}{\partial \theta_l}. \quad (46)$$

In what follows and in Section 5.2.3 we use the general first-order expansion described in Appendix A applied to the product of Jacobian matrices with $\epsilon = 1$.

We rewrite each factor inside the product as

$$M_{j-1} = I + g_{j-1}A_{j-1} + G_{j-1}, \quad (47)$$

where $A_{j-1} = D_{j-1}W^r - I$ and $G_{j-1} = d_{j-1}(J_{j-1}^g)$ is a rank-1 matrix resulting from the outer product of two vectors.

Expanding the product to the first order in the rank-1 corrections G_{j-1} , we obtain

$$\prod_{j=k+1}^t M_{j-1} \approx \underbrace{\prod_{j=k+1}^t (I + g_{j-1}A_{j-1})}_{\text{dominant dynamics}} + \sum_{m=k+1}^t \left(\prod_{j=m+1}^t (I + g_{j-1}A_{j-1}) \right) G_{m-1} \left(\prod_{j=k+1}^{m-1} (I + g_{j-1}A_{j-1}) \right). \quad (48)$$

The first term describes the main dynamics without the rank-1 updates, while the second term is a sum of rank-1 corrections, each inserted at a different time step m and propagated by the full-rank dynamics. We now factor the gate scalars g_{j-1} explicitly from the first term in (48) like we did in Section 5.2.1.

$$\prod_{j=k+1}^t (I + g_{j-1}A_{j-1}) = \left(\prod_{j=k+1}^t g_{j-1} \right) \left(\prod_{j=k+1}^t (g_{j-1}^{-1}I + A_{j-1}) \right).$$

Thus, the gate values contribute as a multiplicative attenuation factor given by the product $\prod_{j=k+1}^t g_{j-1}$, while the remaining matrices describe the dynamics normalized by g_{j-1} . Similarly, the rank-1 corrections remain rank-1 but acquire products of gates from the intervals before and after the insertion of G_{m-1} .

Collecting all terms, we can write

$$\prod_{j=k+1}^t M_{j-1} \approx \left(\prod_{j=k+1}^t g_{j-1} \right) P_{t,k} + \sum_{m=k+1}^t \left(\prod_{j=m+1}^t g_{j-1} \right) R_{t,m} G_{m-1} \left(\prod_{j=k+1}^{m-1} g_{j-1} \right) S_{k,m}, \quad (49)$$

where

$$P_{t,k} = \prod_{j=k+1}^t (g_{j-1}^{-1}I + A_{j-1}),$$

and the normalized matrices $R_{t,m}$ and $S_{k,m}$ are defined as

$$R_{t,m} = \prod_{j=m+1}^t (g_{j-1}^{-1}I + A_{j-1}), \quad S_{k,m} = \prod_{j=k+1}^{m-1} (g_{j-1}^{-1}I + A_{j-1}).$$

Plugging (49) into the gradient expression, we obtain

$$\frac{\partial E_t}{\partial \theta_l} = \frac{\partial E_t}{\partial x_t} \sum_{k=1}^t \left[\left(\prod_{j=k+1}^t g_{j-1} \right) P_{t,k} + \sum_{m=k+1}^t \left(\prod_{j=m+1}^t g_{j-1} \right) R_{t,m} G_{m-1} \left(\prod_{j=k+1}^{m-1} g_{j-1} \right) S_{k,m} \right] \frac{\partial x_k}{\partial \theta_l}. \quad (50)$$

Unlike the constant gate case, here the gates g_{j-1} are *time-varying* and driven by the input and state. Therefore, the attenuation factor is not a simple power (as with α), but a *product of gate values* along the time interval $[k+1, t]$. This product leads to the following effective learning rate:

$$\mu_{t,k}^* = \mu \prod_{j=k+1}^t g_{j-1}, \quad (51)$$

where $\mu_{t,k}^*$ depends on the entire input-driven trajectory of the gates. The additional rank-1 terms capture further corrections due to the gating mechanism, modulating the propagation of gradients in a way that cannot be simplified into a single scalar factor.

5.2.3 RNNs with multiple gates

When considering the Jacobian in (37) the gradient equation becomes:

$$\frac{\partial \mathcal{E}_t}{\partial \theta_l} = \frac{\partial \mathcal{E}_t}{\partial x_t} \sum_{k=1}^t \left[\prod_{j=k+1}^t G_{j-1} + (\hat{g}_{j-1} D_{j-1} W^r) + (\hat{g}_{j-1} I) \right] \frac{\partial x_k}{\partial \theta_l}. \quad (52)$$

Each factor in the product appearing in the gradient expression reads

$$M_{j-1} = \hat{g}_{j-1} I + \hat{g}_{j-1} A_{j-1} + G_{j-1}, \quad (53)$$

where $A_{j-1} = D_{j-1} W^r$, $\Gamma_{j-1} \equiv \hat{g}_{j-1} = \text{diag}(g_{j-1}^{(1)}, \dots, g_{j-1}^{(N_r)})$ is the diagonal matrix of neuron-specific gates and $G_{j-1} = \hat{d}_{j-1} J_{j-1}^g$ is a full-rank matrix in this case.

Unlike the scalar gate case, here \hat{g}_{j-1} does not commute with A_{j-1} , and G_{j-1} is no longer rank-1. Therefore, the factorization is more involved. We can rewrite in terms of perturbation as follows:

$$M_{j-1} = \Gamma_{j-1}(\tilde{A}_{j-1}) + G_{j-1}, \quad (54)$$

where

$$\tilde{A}_{j-1} = A_{j-1} + \Gamma_{j-1}^{-1}(I - \Gamma_{j-1}),$$

with $\Gamma_{j-1}^{-1}(I - \Gamma_{j-1})$ defined element-wise as $\text{diag}((1 - g_{j-1}^{(i)})/g_{j-1}^{(i)})$ for $g_{j-1}^{(i)} > 0$.

Similarly to the scalar gate case, we expand the product to first order in G_{j-1} :

$$\prod_{j=k+1}^t M_{j-1} \approx \underbrace{\prod_{j=k+1}^t (\Gamma_{j-1} \tilde{A}_{j-1})}_{\text{dominant dynamics}} + \sum_{m=k+1}^t \left(\prod_{j=m+1}^t \Gamma_{j-1} \tilde{A}_{j-1} \right) G_{m-1} \left(\prod_{j=k+1}^{m-1} \Gamma_{j-1} \tilde{A}_{j-1} \right). \quad (55)$$

The first term describes the main dynamics through diagonal gates and normalized matrices \tilde{A}_{j-1} . The second term accounts for full-rank corrections due to G_{j-1} .

We now separate the diagonal gate products explicitly:

$$\prod_{j=k+1}^t (\Gamma_{j-1} \tilde{A}_{j-1}) = \left(\prod_{j=k+1}^t \Gamma_{j-1} \right) P_{t,k}, \quad (56)$$

where

$$P_{t,k} = \prod_{j=k+1}^t \tilde{A}_{j-1},$$

and the product $\prod_{j=k+1}^t \Gamma_{j-1}$ is a diagonal matrix with entries

$$\left(\prod_{j=k+1}^t g_{j-1}^{(1)}, \dots, \prod_{j=k+1}^t g_{j-1}^{(N_r)} \right).$$

For the rank corrections, we define

$$R_{t,m} = \prod_{j=m+1}^t \tilde{A}_{j-1}, \quad S_{k,m} = \prod_{j=k+1}^{m-1} \tilde{A}_{j-1}.$$

The full expansion to the first order becomes

$$\prod_{j=k+1}^t M_{j-1} \approx \left(\prod_{j=k+1}^t \Gamma_{j-1} \right) P_{t,k} + \sum_{m=k+1}^t \left(\prod_{j=m+1}^t \Gamma_{j-1} \right) R_{t,m} G_{m-1} \left(\prod_{j=k+1}^{m-1} \Gamma_{j-1} \right) S_{k,m}. \quad (57)$$

Plugging (57) into the gradient formula, we obtain

$$\frac{\partial E_t}{\partial \theta_l} = \frac{\partial E_t}{\partial x_t} \sum_{k=1}^t \left[\left(\prod_{j=k+1}^t \Gamma_{j-1} \right) P_{t,k} + \sum_{m=k+1}^t \left(\prod_{j=m+1}^t \Gamma_{j-1} \right) R_{t,m} G_{m-1} \left(\prod_{j=k+1}^{m-1} \Gamma_{j-1} \right) S_{k,m} \right] \frac{\partial x_k}{\partial \theta_l}. \quad (58)$$

Unlike the scalar gate case, here the gate contributions $\prod_{j=k+1}^t \Gamma_{j-1}$ form a *diagonal matrix* rather than a scalar. Consequently, the attenuation of the gradient is *neuron-specific* and depends on the entire input-driven gate trajectory:

$$\mu_{t,k}^{*(i)} = \mu \prod_{j=k+1}^t g_{j-1}^{(i)}, \quad (59)$$

where $\mu_{t,k}^{*(i)}$ is the effective learning rate for neuron i . This shows that the gating mechanism induces an *anisotropic*, path-dependent scaling of the gradient. For the multi-gate case:

- Each neuron has its own time-varying effective learning rate determined by its gate trajectory.
- The propagation of gradients is anisotropic, with different attenuation along different state-space directions.
- The correction terms involving G_{j-1} are full-rank and cannot be simplified into a low-dimensional form, although their effect is modulated by products of diagonal gate matrices.

Therefore, gating with neuron-specific time scales modulates both the magnitude and directionality of gradient propagation, offering a powerful mechanism for controlling learning dynamics.

6 Gradient descent algorithms

We now turn to well-known variations of the basic gradient descent algorithm [24]. Our goal is to draw parallels between these algorithmic modifications and the implicit effects induced by tunable time scales in RNN state dynamics. In particular, we examine how gates – by shaping the Jacobian structure – alter the effective optimization behaviour of plain gradient descent, in ways reminiscent of learning rate schedules, momentum terms, or adaptive update rules.

6.1 Adam

Adam [15] combines ideas from momentum methods and adaptive learning rate algorithms. Like Adadelta and RMSprop, it maintains an exponentially decaying average of past squared gradients $v_{t,l}$, but it also tracks an exponentially decaying average of past (unsquared) gradients $m_{t,l}$, akin to momentum:

$$m_{t,l} = \beta_1 m_{t,l-1} + (1 - \beta_1) \frac{\partial \mathcal{E}_t}{\partial \theta_l}, \quad (60)$$

$$v_{t,l} = \beta_2 v_{t,l-1} + (1 - \beta_2) \left(\frac{\partial \mathcal{E}_t}{\partial \theta_l} \right)^2, \quad (61)$$

where $\beta_1, \beta_2 \in (0, 1)$ are decay rates, and the squaring in $v_{t,l}$ is applied component-wise.

To correct the initialization bias introduced by these moving averages, Adam computes bias-corrected estimates:

$$\hat{m}_{t,l} = \frac{m_{t,l}}{1 - \beta_1^l}, \quad (62)$$

$$\hat{v}_{t,l} = \frac{v_{t,l}}{1 - \beta_2^l}. \quad (63)$$

The parameter update is then:

$$\theta_{l+1} = \theta_l - \frac{\mu}{b} \sum_{t=1}^b \frac{\hat{m}_{t,l}}{\sqrt{\hat{v}_{t,l} + \epsilon}}, \quad \epsilon > 0, \quad (64)$$

where b is the mini-batch size and ϵ is a small constant to prevent division by zero.

6.2 Analogies between gating mechanisms and adaptive gradient descent methods

The analysis in Sections 5.2.1–5.2.3 shows that the Jacobian factors in gated RNNs naturally lead to multiplicative modulation of the backpropagated gradient. From the first-order expansion, this modulation directly translates into an *effective learning rate* that depends on the gate configuration. This behavior closely parallels well-known adaptive variants of gradient descent.

Constant gate (α). In the constant-gate (leaky integrator) case, the gate value $\alpha \in (0, 1]$ is fixed throughout training and across all units. The dominant multiplicative factor in the backward product over $(t - k)$ steps is α^{t-k} , independent of the input sequence or hidden state trajectory. Unlike the time-varying or multi-gate cases, there is no data dependence: the scaling depends solely on $(t - k)$ and α , remaining fixed during training. This is analogous to a fixed preconditioning factor in gradient descent, where every parameter update is scaled by the same precomputed value.

Single time-varying gate (g_{j-1}). With a scalar gate g_{j-1} , the effective learning rate becomes

$$\mu_{t,k}^* = \mu \prod_{j=k+1}^t g_{j-1}.$$

Here, the gradient is modulated by a global, input-driven attenuation factor that varies over time. This is conceptually similar to a learning rate schedule (e.g., exponential decay), with the key difference that the modulation emerges from the network's own state dynamics rather than from an externally prescribed schedule.

Multiple time-varying gates ($g_{j-1}^{(i)}$). In the multi-gate case, the modulation is neuron-specific:

$$\mu_{t,k}^{*(i)} = \mu \prod_{j=k+1}^t g_{j-1}^{(i)},$$

so each neuron i has its own effective learning rate, determined by the trajectory of its gate values. This mirrors adaptive optimizers such as Adam or RMSProp, which assign each parameter a distinct, dynamically adjusted step size.

Corrections due to G_{j-1} . The additional G_{j-1} terms, which arise naturally in the first-order expansion, introduce directional modifications to the gradient. In the single-gate case, these corrections are rank-1, acting as low-dimensional perturbations akin to momentum. In the multi-gate case, G_{j-1} is full-rank, leading to anisotropic scaling reminiscent of the preconditioning performed by Adam and other second-order adaptive methods.

Gating case	Gradient modulation	Analogy with optimizers
Constant gate (α)	Fixed scaling depending on distance ($t - k$)	SGD with a constant, precomputed scaling factor
Time-varying scalar gate (g_{j-1})	Global, input-driven scaling over time	SGD with a learning rate schedule
Multiple gates ($g_{j-1}^{(i)}$)	Per-neuron (diagonal) scaling	Adam/RMSProp (per-parameter adaptation)
Corrections (G_{j-1})	Directional modulation (rank-1 or full-rank)	Momentum / adaptive preconditioning

Table 1: Conceptual similarities between gating-induced gradient modulation and adaptive gradient descent methods.

In summary, the presence of gates in RNN dynamics not only stabilizes gradient propagation across long sequences but also induces implicit, data-driven modulation of the effective learning rate. Depending on the gating configuration, this modulation can behave like a fixed preconditioner, a dynamic learning rate schedule, or a fully adaptive per-parameter step size—mirroring the design principles of modern optimization algorithms without explicitly modifying the optimizer.

7 Conclusions and future directions

In this work, we have introduced a theoretical framework that couples the time scales of state-space dynamics with the parameter-space dynamics of recurrent neural networks. By modeling gating mechanisms as parametrized modifiers of state transitions, we demonstrated that their influence extends beyond state evolution: gates implicitly induce *adaptive learning-rate behavior* in parameter updates, even when training is carried out with a fixed global learning rate. Through a first-order Fréchet expansion of Jacobian products, we established how these gate-induced effects alter gradient propagation, scale step sizes, and introduce anisotropy in parameter updates.

Our derivations show that the corrections induced by gates can be treated as small, structured perturbations of the dominant dynamics in many practical regimes. Numerical experiments with constant, scalar, and multi-dimensional gates validated this approximation, confirming both the smallness of the corrections and the accuracy of the predicted scaling laws, even at the operating point $\varepsilon = 1$.

Taken together, these results provide a unified dynamical-systems perspective on gating: gates serve not only as state filters but also as intrinsic mechanisms for adaptive optimization, effectively bridging state-space time scales and parameter-space learning dynamics. This perspective also highlights that adaptive learning-rate methods such as Adam or RMSprop could be revisited in light of these findings: rather than treating

optimization and gating as separate mechanisms, future adaptive methods might explicitly incorporate the time-scale interactions revealed here, potentially leading to simpler or more principled training strategies.

Future work will extend this analysis to more advanced gated architectures such as LSTMs and GRUs, as well as modern sequence models with multiplicative interactions. We also plan to investigate the role of these time-scale interactions in tasks with long-range temporal dependencies, and to explore how the framework can guide the principled design of novel architectures that combine stability, training efficiency, and interpretability.

A Matrix product expansion via the Fréchet derivative formulation

We derive here the first-order expansion of a product of matrices with structured perturbations, starting from the *product rule for the Fréchet derivative* (Theorem 3.3 in Higham [11]). We also show how the same reasoning yields higher-order terms.

A.1 Fréchet Differentiability and the First-Order Expansion

Let $\mathbb{C}^{n \times n}$ denote the finite-dimensional vector space of complex $n \times n$ matrices equipped with a matrix norm (specifically, the operator 2-norm, unless otherwise stated). Since the space is finite-dimensional, all norms are equivalent, but fixing a concrete norm allows us to quantify perturbations in a consistent way.

Definition A.1 (Fréchet differentiability [11, Def. 3.1]). Let $f : \mathbb{C}^{n \times n} \rightarrow \mathbb{C}^{n \times n}$. We say that f is *Fréchet differentiable* at $A \in \mathbb{C}^{n \times n}$ if there exists a bounded linear mapping

$$L_f(A, \cdot) : \mathbb{C}^{n \times n} \rightarrow \mathbb{C}^{n \times n}$$

such that

$$\lim_{\|E\| \rightarrow 0} \frac{\|f(A + E) - f(A) - L_f(A, E)\|}{\|E\|} = 0. \quad (65)$$

The operator $L_f(A, \cdot)$ is called the *Fréchet derivative* of f at A , and it is unique if it exists.

Intuitively, $L_f(A, \cdot)$ provides the best linear approximation to f near A ; for functions between finite-dimensional normed spaces, this is equivalent to the existence of the Gâteaux derivative that is uniformly continuous in a neighbourhood of A [11, Sec. 3.1].

First-order expansion. If f is Fréchet differentiable at A , the first-order Taylor expansion reads

$$f(A + E) = f(A) + L_f(A, E) + o(\|E\|), \quad (66)$$

where $E \in \mathbb{C}^{n \times n}$ is the *perturbation matrix*, specifying the direction and structure of the infinitesimal change applied to A . The notation $o(\|E\|)$ means that $\|o(\|E\|)\|/\|E\| \rightarrow 0$ as $\|E\| \rightarrow 0$.

Product rule. If g and h are Fréchet differentiable at A , their product $f(X) = g(X)h(X)$ satisfies the *product rule*:

$$L_{gh}(A, E) = L_g(A, E)h(A) + g(A)L_h(A, E), \quad (67)$$

where $L_g(A, E)$ denotes the Fréchet derivative of g at A in the direction E ; see [11, Sec. 3.2, Thm. 3.3] for a proof.

A.2 Matrix products with structured perturbations

We now consider a product of n factors, each with a perturbation proportional to a scalar parameter ε :

$$F(\varepsilon) = \prod_{j=1}^n (A_j + \varepsilon B_j), \quad (68)$$

where:

- $A_j \in \mathbb{C}^{d \times d}$ is the *unperturbed* factor at position j ,
- $B_j \in \mathbb{C}^{d \times d}$ is the *perturbation* at position j ,
- $\varepsilon \in \mathbb{R}$ controls the magnitude of all perturbations.

The direction of perturbation E in (66) is now the tuple

$$E \equiv (B_1, B_2, \dots, B_n),$$

meaning that in slot j the perturbation is B_j while all other slots are unchanged. Since each factor in (68) is affine in ε , $F(\varepsilon)$ is a polynomial in ε of degree at most n .

A.3 Recursive application of the product rule

For any $k \leq n, \varepsilon > 0$, define the product

$$F_k(\varepsilon) := \prod_{j=1}^k (A_j + \varepsilon B_j), \quad \text{so that} \quad F_n(\varepsilon) = F_{n-1}(\varepsilon) (A_n + \varepsilon B_n).$$

We now apply the product rule (67) to F_n by setting

$$g(\varepsilon) = F_{n-1}(\varepsilon), \quad h(\varepsilon) = A_n + \varepsilon B_n.$$

At $\varepsilon = 0$ we have:

$$g(0) = F_{n-1}(0) = A_1 A_2 \dots A_{n-1}, \quad h(0) = A_n, \quad L_h(0, E) = B_n.$$

The product rule gives:

$$L_{F_n}(0, E) = L_g(0, E) A_n + (A_1 \dots A_{n-1}) B_n. \quad (69)$$

- The first term *passes the derivative back* into the earlier factors F_{n-1} , leaving A_n unperturbed.
- The second term keeps the first $n - 1$ factors unperturbed and inserts the perturbation B_n in the last position.

By continuing this recursion for general n , we obtain the following first-order Fréchet derivative

$$L_{F_n}(0, E) = \sum_{i=1}^n \left(\prod_{j=1}^{i-1} A_j \right) B_i \left(\prod_{j=i+1}^n A_j \right), \quad (70)$$

where the empty product is taken to be the identity matrix.

Illustration for $n = 3$ Write

$$F_3(\varepsilon) = (A_1 + \varepsilon B_1)(A_2 + \varepsilon B_2)(A_3 + \varepsilon B_3), \quad F_2(\varepsilon) = (A_1 + \varepsilon B_1)(A_2 + \varepsilon B_2), \quad F_1(\varepsilon) = A_1 + \varepsilon B_1,$$

and take the perturbation direction to be the tuple $E = (B_1, B_2, B_3)$.

Step 1 (apply product rule to F_3). Set

$$g(\varepsilon) = F_2(\varepsilon), \quad h(\varepsilon) = A_3 + \varepsilon B_3.$$

Then at $\varepsilon = 0$:

$$g(0) = F_2(0) = A_1 A_2, \quad h(0) = A_3, \quad L_h(0, E) = B_3.$$

Using (67),

$$L_{F_3}(0, E) = L_g(0, E) h(0) + g(0) L_h(0, E) = L_{F_2}(0, E) A_3 + (A_1 A_2) B_3. \quad (71)$$

Step 2 (expand $L_{F_2}(0, E)$). Apply the product rule to F_2 by setting

$$g(\varepsilon) = F_1(\varepsilon), \quad h(\varepsilon) = A_2 + \varepsilon B_2.$$

Then at $\varepsilon = 0$:

$$g(0) = F_1(0) = A_1, \quad h(0) = A_2, \quad L_h(0, E) = B_2.$$

Hence

$$L_{F_2}(0, E) = L_{F_1}(0, E) A_2 + A_1 B_2. \quad (72)$$

Step 3 (expand $L_{F_1}(0, E)$). Here $F_1(\varepsilon) = A_1 + \varepsilon B_1$ is a single affine factor, so

$$L_{F_1}(0, E) = B_1. \quad (73)$$

Assemble. Substitute (72) into (71), and then use (73):

$$\begin{aligned} L_{F_3}(0, E) &= (L_{F_1}(0, E) A_2 + A_1 B_2) A_3 + (A_1 A_2) B_3 \\ &= (B_1 A_2) A_3 + (A_1 B_2) A_3 + A_1 A_2 B_3 \\ &= B_1 A_2 A_3 + A_1 B_2 A_3 + A_1 A_2 B_3. \end{aligned}$$

Thus each term contains exactly one perturbation B_i in position i , with all other slots occupied by their unperturbed counterparts A_j .

A.4 First-order expansion

Applying the first-order Taylor expansion (66) to (68) gives

$$F(\varepsilon) = F(0) + \varepsilon L_F(0, E) + O(\varepsilon^2), \quad (74)$$

where $F(0) = \prod_{j=1}^n A_j$ and $L_F(0, E)$ is given by (70). Substituting, we obtain the explicit first-order expansion:

$$F(\varepsilon) = \left(\prod_{j=1}^n A_j \right) + \varepsilon \sum_{m=1}^n \left(\prod_{j=m+1}^n A_j \right) B_m \left(\prod_{j=1}^{m-1} A_j \right) + O(\varepsilon^2). \quad (75)$$

Higher-order terms The same idea applies to higher derivatives: an r -th order term comes from choosing exactly r distinct slots for the perturbations B . The general r -th Fréchet derivative at $\varepsilon = 0$ is

$$F^{(r)}(0) = r! \sum_{1 \leq m_1 < \dots < m_r \leq n} \left(\prod_{j=m_r+1}^n A_j \right) B_{m_r} \left(\prod_{j=m_{r-1}+1}^{m_r-1} A_j \right) B_{m_{r-1}} \cdots B_{m_1} \left(\prod_{j=1}^{m_1-1} A_j \right). \quad (76)$$

Thus the exact Taylor expansion (terminating at degree n) is

$$F(\varepsilon) = \sum_{r=0}^n \frac{\varepsilon^r}{r!} F^{(r)}(0). \quad (77)$$

Note that $F^{(1)}(0) \equiv L_F(0, E)$.

A.5 Simulations supporting the validity of the first-order approximation

The first-order expansion (75) is accurate when all $\|B_j\|$ are small compared to $\|A_j\|$ (in operator norm), so that the accumulated $O(\varepsilon^2)$ terms remain negligible. In the main text, B_j represents gate-induced corrections, which are typically low-norm compared to the dominant dynamics in A_j . To support the validity of the expansion (75) in our setting, we perform numerical checks on the Jacobian factors extracted from the RNN models considered. Two complementary diagnostics are used: (i) for a range of ε values, we evaluate the truncation error

$$\|F(\varepsilon) - [F(0) + \varepsilon L_F(0, B)]\|$$

and verify that it scales as $O(\varepsilon^2)$, as predicted by the theory; (ii) in the operating regime of the paper ($\varepsilon = 1$), we measure the per-step operator-norm ratio $r_j = \|B_j\|_2/\|A_j\|_2$ over the time horizon. The first diagnostic confirms the expected order of accuracy of the expansion, while the second verifies that the B_j terms remain small compared to A_j in practice, ensuring that the neglected $O(\varepsilon^2)$ contributions are indeed negligible even at $\varepsilon = 1$.

Scalar gate case

Figures 1–4 report the results for the single scalar gate configuration. The truncation error in Fig. 1 follows a clear ε^2 scaling across the entire range up to $\varepsilon = 1$, indicating that the first-order expansion maintains second-order accuracy even in the actual operating regime of the network. The corresponding second-order remainder $C_2(\varepsilon) = \|F - T_1\|/\varepsilon^2$ (Fig. 2) approaches a constant for small ε and stays extremely small for ε near 1, showing that higher-order contributions are negligible in practice.

The per-step Jacobian norm comparison in Fig. 3 shows that gate corrections B_j are consistently an order of magnitude smaller than the dominant A_j terms, with the ratio distribution in Fig. 4 tightly concentrated below 0.1. This confirms that the smallness condition $\|B_j\| \ll \|A_j\|$ holds well throughout the sequence, even in the $\varepsilon = 1$ regime.

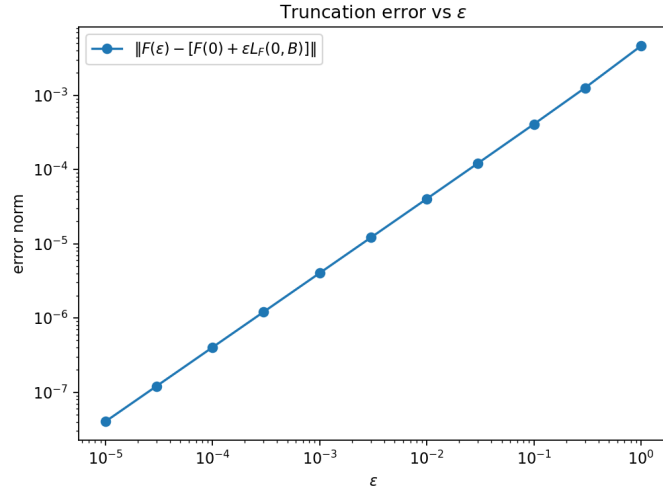


Figure 1: First-order truncation error vs. ε for the scalar gate case.

Multi-gate case

Figures 5–8 show the corresponding diagnostics for the multi-gate configuration. The truncation error in Fig. 5 also follows the predicted ε^2 scaling across the full range up to $\varepsilon = 1$, with no significant loss of accuracy in the large- ε regime relevant to our models. The second-order remainder $C_2(\varepsilon)$ in Fig. 6 flattens

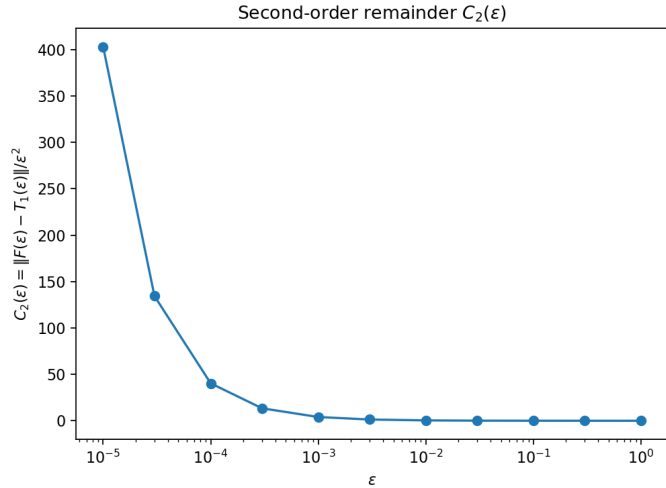


Figure 2: Second-order remainder $C_2(\varepsilon)$ for the scalar gate case.

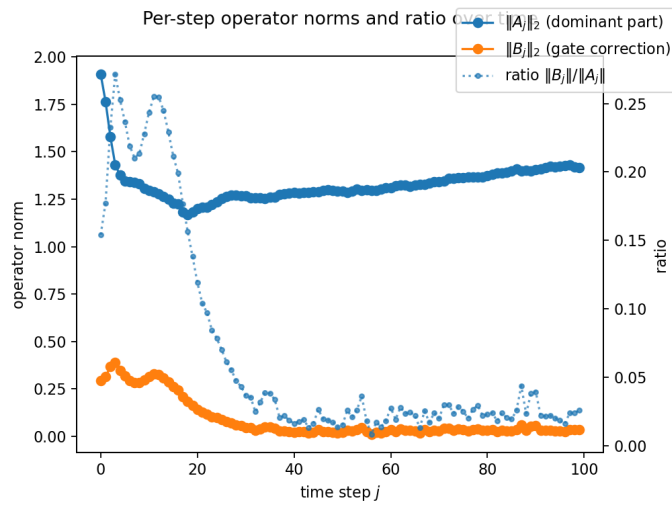


Figure 3: Per-step norms $\|A_j\|_2$ (dominant part), $\|B_j\|_2$ (gate correction), and their ratio over time for the scalar gate case.

to a constant in the small- ε limit and remains very small for $\varepsilon = 1$, again indicating that neglected higher-order terms are practically irrelevant.

The per-step norm analysis in Fig. 7 confirms that gate corrections B_j are consistently small compared to A_j , with the ratio distribution in Fig. 8 concentrated well below 0.1. These results demonstrate that the smallness condition $\|B_j\| \ll \|A_j\|$ is robustly satisfied in the multi-gate case as well, validating the use of the first-order expansion in both architectures studied.

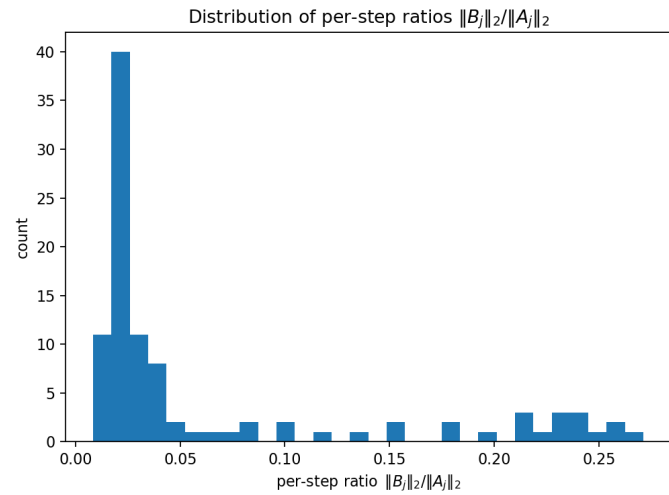


Figure 4: Distribution of per-step ratios $\|B_j\|_2/\|A_j\|_2$ for the scalar gate case.

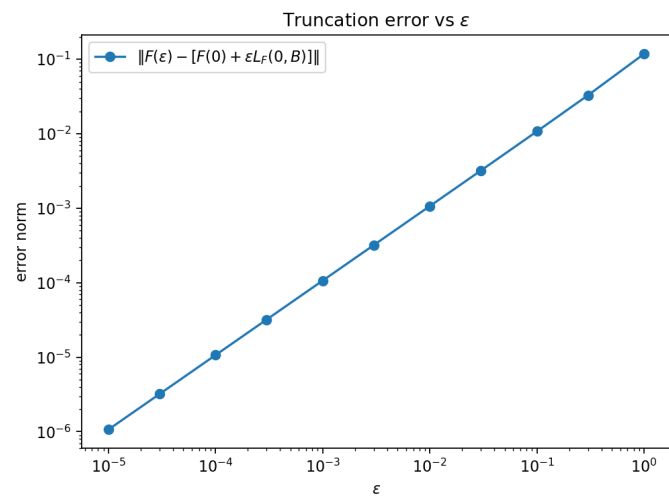


Figure 5: First-order truncation error vs. ε for the multi-gate case.

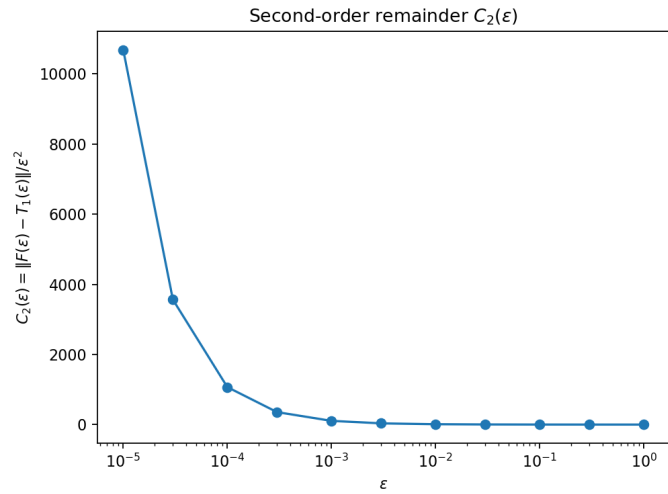


Figure 6: Second-order remainder $C_2(\varepsilon)$ for the multi-gate case.

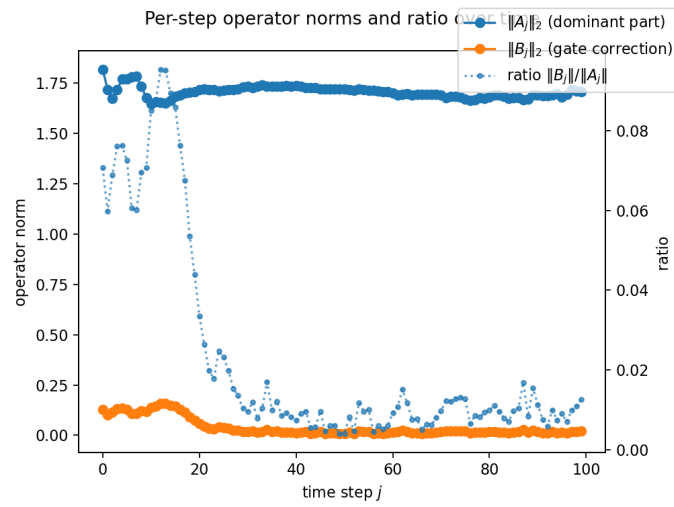


Figure 7: Per-step norms $\|A_j\|_2$ (dominant part), $\|B_j\|_2$ (gate correction), and their ratio over time for the multi-gate case.

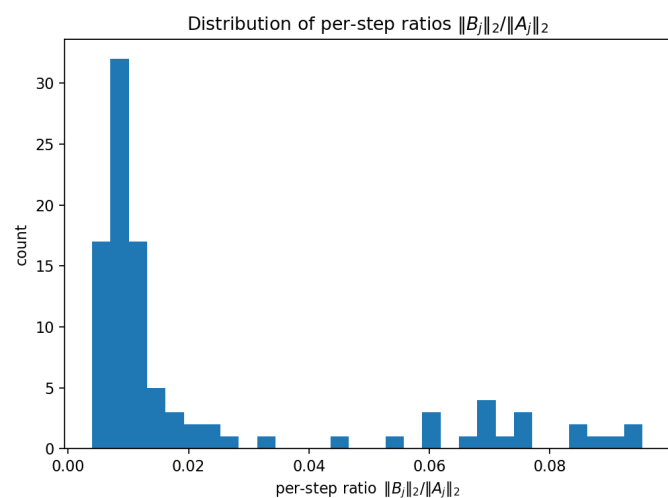


Figure 8: Distribution of per-step ratios $\|B_j\|_2/\|A_j\|_2$ for the multi-gate case.

References

- [1] M. Arjovsky, A. Shah, and Y. Bengio. Unitary evolution recurrent neural networks. In *International Conference on Machine Learning*, pages 1120–1128, New York, USA, June 2016.
- [2] O. Can, K. Kapanova, and A. Søgaard. Gates create slow modes in recurrent neural networks. In *International Conference on Learning Representations (ICLR)*, 2020.
- [3] A. Cen. Random orthogonal additive filters: A solution to the vanishing/exploding gradient of deep neural networks. *IEEE Transactions on Neural Networks and Learning Systems*, 36(6):10794–10807, 2025. doi: 10.1109/TNNLS.2025.3538924.
- [4] B. Chang, M. Chen, E. Haber, and E. H. Chi. AntisymmetricRNN: A dynamical system view on recurrent neural networks. In *International Conference on Learning Representations*, 2019. URL <https://openreview.net/forum?id=ryxepo0cFX>.
- [5] M. Chen, J. Pennington, and S. Schoenholz. Dynamical isometry and a mean field theory of RNNs: Gating enables signal propagation in recurrent neural networks. In J. Dy and A. Krause, editors, *Proceedings of the 35th International Conference on Machine Learning*, volume 80 of *Proceedings of Machine Learning Research*, pages 873–882, Stockholm, Sweden, 10–15 Jul 2018. PMLR.
- [6] N. B. Erichson, O. Azencot, A. Queiruga, L. Hodgkinson, and M. W. Mahoney. Lipschitz recurrent neural networks. *arXiv preprint arXiv:2006.12070*, 2021.
- [7] D. Gilboa, B. Chang, M. Chen, G. Yang, S. S. Schoenholz, E. H. Chi, and J. Pennington. Dynamical isometry and a mean field theory of lstms and grus. *arXiv preprint arXiv:1901.08987*, 2019.
- [8] A. Gu, K. Goel, and C. Ré. Efficiently modeling long sequences with structured state spaces. *arXiv preprint arXiv:2111.00396*, 2021.
- [9] A. Gu, I. Johnson, K. Goel, K. K. Saab, T. Dao, A. Rudra, and C. Ré. Combining recurrent, convolutional, and continuous-time models with linear state space layers. In *Thirty-Fifth Conference on Neural Information Processing Systems*, 2021.
- [10] K. Helfrich, D. Willmott, and Q. Ye. Orthogonal recurrent neural networks with scaled Cayley transform. In J. Dy and A. Krause, editors, *Proceedings of the 35th International Conference on Machine Learning*, volume 80 of *Proceedings of Machine Learning Research*, pages 1969–1978. PMLR, 10–15 Jul 2018.
- [11] N. J. Higham. *Functions of Matrices: Theory and Computation*. SIAM, 2008.
- [12] H. Jaeger, M. Lukoševičius, D. Popovici, and U. Siewert. Optimization and applications of echo state networks with leaky-integrator neurons. *Neural Networks*, 20(3):335–352, 2007. doi: 10.1016/j.neunet.2007.04.016.
- [13] A. Kag, Z. Zhang, and V. Saligrama. RNNs incrementally evolving on an equilibrium manifold: A panacea for vanishing and exploding gradients? In *International Conference on Learning Representations*, 2020.
- [14] G. Kerg, K. Goyette, M. P. Touzel, G. Gidel, E. Vorontsov, Y. Bengio, and G. Lajoie. Non-normal recurrent neural network (nnrnn): learning long time dependencies while improving expressivity with transient dynamics. *arXiv preprint arXiv:1905.12080*, 2019.
- [15] D. Kingma and J. Ba. Adam: A method for stochastic optimization. *arXiv preprint arXiv:1412.6980*, 2014.

[16] J. Koutnik, K. Greff, F. Gomez, and J. Schmidhuber. A clockwork RNN. In *International Conference on Machine Learning*, volume 32, pages 1863–1871, 2014.

[17] A. Krishnamurthy, C. Gehring, D. K. Misra, and C. Zhang. Theory of gating in recurrent neural networks. *Journal of Machine Learning Research*, 23(157):1–39, 2022.

[18] J. Lee, L. Xiao, S. Schoenholz, Y. Bahri, R. Novak, J. Sohl-Dickstein, and J. Pennington. Wide neural networks of any depth evolve as linear models under gradient descent. *Advances in neural information processing systems*, 32, 2019.

[19] Z. Mhammedi, A. Hellicar, A. Rahman, and J. Bailey. Efficient orthogonal parametrisation of recurrent neural networks using householder reflections. In *Proceedings of the 34th International Conference on Machine Learning*, page 2401–2409, 2017.

[20] N. Muca Cirone, A. Orvieto, B. Walker, C. Salvi, and T. Lyons. Theoretical foundations of deep selective state-space models. *Advances in Neural Information Processing Systems*, 37:127226–127272, 2024.

[21] R. Pascanu, T. Mikolov, and Y. Bengio. On the difficulty of training recurrent neural networks. In *Proceedings of the 30th International Conference on Machine Learning*, volume 28, pages 1310–1318, Atlanta, Georgia, USA, 2013.

[22] J. Pennington, S. Schoenholz, and S. Ganguli. Resurrecting the sigmoid in deep learning through dynamical isometry: theory and practice. In *Advances in Neural Information Processing Systems*, pages 4785–4795, 2017.

[23] R. Quax, D. Kandhai, and P. M. A. Sloot. Adaptive time scales in recurrent neural networks. *Scientific Reports*, 10(1):7442, 2020.

[24] S. Ruder. An overview of gradient descent optimization algorithms. *arXiv preprint arXiv:1609.04747*, 2016.

[25] T. K. Rusch and S. Mishra. Coupled oscillatory recurrent neural network (cornn): An accurate and (gradient) stable architecture for learning long time dependencies. *ICLR*, 2021.

[26] T. K. Rusch, S. Mishra, N. B. Erichson, and M. W. Mahoney. Long expressive memory for sequence modeling. *arXiv preprint arXiv:2110.04744*, 2021.

[27] A. M. Saxe, J. L. McClelland, and S. Ganguli. Exact solutions to the nonlinear dynamics of learning in deep linear neural networks. *arXiv preprint arXiv:1312.6120*, 2013.

[28] C. Tallec and Y. Ollivier. Can recurrent neural networks warp time? In *International Conference on Learning Representations*, 2018. URL <https://openreview.net/forum?id=SJcKhk-Ab>.

[29] M. O. Turkoglu, S. D’Aronco, J. D. Wegner, and K. Schindler. Gating revisited: Deep multi-layer rnns that can be trained. *IEEE Transactions on Pattern Analysis and Machine Intelligence*, 44(8):4081–4092, 2022. doi: 10.1109/TPAMI.2021.3064878.

[30] J. Van Der Westhuizen and J. Lasenby. The unreasonable effectiveness of the forget gate. *arXiv preprint arXiv:1804.04849*, 2018.

[31] E. Vorontsov, C. Trabelsi, S. Kadoury, and C. Pal. On orthogonality and learning recurrent networks with long term dependencies. In *Proceedings of the 34th International Conference on Machine Learning*, page 3570–3578, 2017.

[32] P. J. Werbos. Backpropagation through time: what it does and how to do it. *Proceedings of the IEEE*, 78(10):1550–1560, 1990.

- [33] S. Wisdom, T. Powers, J. Hershey, J. Le Roux, and L. Atlas. Full-capacity unitary recurrent neural networks. In D. D. Lee, M. Sugiyama, U. V. Luxburg, I. Guyon, and R. Garnett, editors, *Advances in Neural Information Processing Systems*, pages 4880–4888. Curran Associates, Inc., Barcelona, Spain, Dec. 2016.
- [34] N. Zucchet and A. Orvieto. Recurrent neural networks: vanishing and exploding gradients are not the end of the story. *Advances in Neural Information Processing Systems*, 37:139402–139443, 2024.